



NRC Publications Archive Archives des publications du CNRC

Copper tungstate thin-films for nitric oxide sensing

Gonzalez, C. M.; Du, X.; Dunford, J. L.; Post, M. L.

This publication could be one of several versions: author's original, accepted manuscript or the publisher's version. /
La version de cette publication peut être l'une des suivantes : la version prépublication de l'auteur, la version
acceptée du manuscrit ou la version de l'éditeur.

For the publisher's version, please access the DOI link below. / Pour consulter la version de l'éditeur, utilisez le lien
DOI ci-dessous.

Publisher's version / Version de l'éditeur:

<https://doi.org/10.1016/j.snb.2012.06.067>

Sensors and Actuators B: Chemical, 173, pp. 169-176, 2012-07-08

NRC Publications Record / Notice d'Archives des publications de CNRC:

<https://nrc-publications.canada.ca/eng/view/object/?id=91216a28-404e-4d8c-809a-1dc56372b15f>

<https://publications-cnrc.canada.ca/fra/voir/objet/?id=91216a28-404e-4d8c-809a-1dc56372b15f>

Access and use of this website and the material on it are subject to the Terms and Conditions set forth at

<https://nrc-publications.canada.ca/eng/copyright>

READ THESE TERMS AND CONDITIONS CAREFULLY BEFORE USING THIS WEBSITE.

L'accès à ce site Web et l'utilisation de son contenu sont assujettis aux conditions présentées dans le site

<https://publications-cnrc.canada.ca/fra/droits>

LISEZ CES CONDITIONS ATTENTIVEMENT AVANT D'UTILISER CE SITE WEB.

Questions? Contact the NRC Publications Archive team at

PublicationsArchive-ArchivesPublications@nrc-cnrc.gc.ca. If you wish to email the authors directly, please see the
first page of the publication for their contact information.

Vous avez des questions? Nous pouvons vous aider. Pour communiquer directement avec un auteur, consultez la
première page de la revue dans laquelle son article a été publié afin de trouver ses coordonnées. Si vous n'arrivez
pas à les repérer, communiquez avec nous à PublicationsArchive-ArchivesPublications@nrc-cnrc.gc.ca.



Copper Tungstate Thin-Films for Nitric Oxide Sensing

C. M. Gonzalez, X. Du, J. L. Dunford and M.L. Post

Institute for Chemical Process and Environmental Technology, National Research Council of Canada,

1200 Montreal Road, Ottawa, Ontario, K1A 0R6, Canada.

Abstract:

CuWO₄ thin-films prepared by the pulsed laser deposition technique were studied for monitoring nitric oxide (NO) in the concentration range $10 < [\text{NO}] < 400$ ppm under synthetic air. The thin-film films were characterized by X-ray diffraction (XRD), depth-profilometry and electron transport measurements. The CuWO₄ thin-film response to O₂ confirmed an n-type conductivity. Monitoring the thin-film conductometric response to NO at both 300 and 500 °C revealed the operation of a temperature-dependent mechanism for detection. At 300 °C, increasing [NO] produced a consistent increment in thin-film resistance, while at 500 °C the thin-film resistance decreased with [NO]. At 500 °C, a transient response was systematically observed. The chemical origin of the transient is discussed. The estimation of response factors to NO exposure in the presence of high [O₂] indicates a significantly higher selectivity to NO. Extensive conductometric measurements show that the thin-films feature good electronic and thermal stability over time.

Conductometric Gas Sensors. NO_x sensors. Environment Monitoring Technologies. Semiconductor Metal Oxides.

1. Introduction

Nitrogen oxides (NO_x) comprise a family of gas-phase species, some of which are recognised as particularly noxious pollutants (*e.g.* NO and NO_2) [1]. Of these compounds, nitrogen monoxide (NO) and nitrogen dioxide (NO_2) are primarily formed from fossil fuel combustion, and these can promote the formation of derived nitrogen oxides such as N_2O , N_2O_2 , N_2O_3 and N_2O_4 , as well as nitric (HNO_3) and nitrous (HNO_2) acids, particulate matter and ozone (O_3). Human exposure to NO at sub-ppm concentrations is found to produce conjunctivitis and dermatitis, and to irritate mucous membranes, including sinuses, pharynx and bronchia. Prolonged exposure has been linked to irregular respiration and pulmonary edema. The exposure limits set by most jurisdictions (*e.g.* NIOSH REL) is 25ppm, and the level of immediate danger to life or health (IDLH) is 100ppm.

In conventional gasoline automobiles, the fuel-rich nature of the combustible mixture can reduce the production of NO_x species due to the presence of O_2 in lower concentration than that required for full combustion. Because of this set of operational conditions, the rich composition of the combustion mixture results in the emission of high amounts of CO and hydrocarbons. In contrast, when diesel engines are operated at an oxygen concentration in the stoichiometric range, the combustion process results in the efficient consumption of fuels and in a dramatic reduction of levels of CO . Nonetheless, these operating conditions produce a large amount of CO_2 and promotes the formation of NO and NO_2 . The increasing popularity of diesel vehicles (and lean burn automobile systems), given their superior power and higher efficiency per unit of fuel volume, has produced a fast increase in the atmospheric levels of NO_x gases and other associated pollutants [1]. Typical concentrations of emitted NO can range from very low ppm levels to a few hundreds of ppm. However, under transient high load conditions or in cases where combustion efficiency is compromised, emissions levels up to 1000ppm or higher can occur. With the increase of functioning diesel automobiles, government institutions around the globe have initiated regulatory legislations to control NO_x emissions [2]. The implementation of these legislations has pressured the automobile

industry to produce more reliable, selective and robust NO_x sensors for use in engine emissions control and for monitoring the operational effectiveness of exhaust stream conditioning systems.

Currently, the technology applied to NO_x monitoring in automobile exhausts comprises the λ -sensor design (amperometric sensor). The working principle is based on the measurement of the O₂ concentration in both a reference system (up-stream to the catalytic treatment where this is present) and in the after-treatment exhaust. This sensor prototype requires the use of an additional reference electrode. Thus, the concentration of NO_x gases is not estimated by the direct detection of NO_x species. An alternative approach for the design of compact and reliable NO_x sensors with good performance, involves the use of semiconducting metal-oxide thin-films as the sensing phase [3-5]. Such sensors can be suitable for a wide range of monitoring applications (including NO_x monitoring in automobile emissions) in a variety of NO_x emitting systems: biological systems, small engines, electricity generators, as well as in agricultural, non-road and industrial applications (*e.g.* air quality control technologies). The sensor detection mechanism is based on surface interactions between semiconductor surface-states (*e.g.* free electrons, vacancies, empty orbitals or holes and oxygen adsorbates) and a gas-phase analyte. The effect of such interactions on the sensing material electron transport properties is interpreted and quantified through changes in conductivity (or measured conductance). Moreover, a semiconducting metal-oxide offers the possibility of miniaturization for the sensing phase (*e.g.* thin-films), reaching the nanoscopic size-scale. This constitutes a practical means for the realization of sensor devices with superior performance since the nanometric dimensions of the sensing film provide an enhanced response to a diversity of physicochemical stimuli (temperature, mass changes, vibrations, magnetic fields, UV-UVvis radiation) and chemical environments (effect of chemical interactions with surrounding analytes, reactivity and chemical affinity, concentration effects, humidity), as well as for cost reduction. Nanometric films of the type used here can be reliably deposited by the pulsed laser deposition technique (PLD). This technique offers an approach to enhance sensor functionality by controlled and reproducible nanostructure manipulations, depending on the laser ablation parameters (*e.g.* laser ablation time, pulse energy,

pulse frequency) and the deposition chamber parameters, such as background O₂ pressure in the case of metal oxides, and also substrate temperature which can promote desirable structural features such as preferential orientation.

Previous studies have shown that WO₃ is a material highly suited for the real-time monitoring of gas-phase pollutants (conductometric sensing phase), particularly for NO_x monitoring [6-14]. Specifically, two major strategies have been used to improve sensor performance: *i*) WO₃ in combination with catalytic metals [8-10] and *ii*) metal-oxide composite formulations with the use of a metal-oxide cocatalyst [11-14]. The present work reports the latter as the experimental strategy to enhance the sensing profile of WO₃, specifically using novel (CuWO₄) thin-films.

Thin-films were prepared using the pulsed laser deposition technique (PLD). The crystallographic and structural features of the CuWO₄ thin-films are discussed and the temperature effect on the electron transport properties of the thin-films upon exposure to O₂ and NO was investigated. Sensing performance towards O₂ and NO was evaluated in ranges commonly expected in automobile exhaust emissions.

2. Materials and Methods

CuWO₄ was prepared by a solid-state reaction between WO₃ and CuO at high temperature. The reagents, WO₃ (Alfa Aesar, 99.998 %) and CuO (Alfa Aesar, 99.995 %), were used as received. A mixture of CuO and WO₃ with 1 : 1 stoichiometric molar ratio was placed in an alumina crucible and sintered in two steps under a flowing oxygen atmosphere. First, the metal oxides were allowed to react at 600 °C for 12 hours. Prior to a second thermal treatment, the resulting material was thoroughly ground and the resulting powder sintered under O₂ at 750 °C for an additional 24 hours.

A target in the form of a compact pellet with size 12 mm (diameter) x 5 mm (thickness) was used for the preparation of thin-films using the pulsed laser ablation deposition technique (PLD). The PLD target was prepared using the powder resulting from the procedure described above by isostatic pressing at 2 T in a mould. The pellet was sintered at 680 °C for 24 hours in O₂.

Thin-films of CuWO_4 were produced using a Lambda Physik LPX305i laser operating at $\lambda = 248$ nm and an atmosphere / vacuum controlled deposition chamber. The films were deposited on single crystal sapphire substrates, $\alpha\text{-Al}_2\text{O}_3$ ($1\bar{1}02$), using a laser ablation period of 20 minutes at a pulse rate and energy of 8Hz and 600 mJ, respectively. During the ablation period, the substrate was isothermal at $T = 600$ °C and the pressure of O_2 was 100 mtorr. Following deposition, the chamber pressure was increased to $p(\text{O}_2) = 400$ Torr and the films were kept at $T = 600$ °C for 30 minutes. Finally, the thin-films were cooled to 25 °C at a rate of ~ 8 °C / minute.

2.1 Physicochemical Characterization

Laser targets and CuWO_4 thin-films were characterized by powder X-ray diffraction (P-XRD) using a Bruker-D8 diffractometer with parallel beam geometry and a sample holder kept stationary with both the XR-source tube and detector arms mobile. The XR-source was a cobalt anode ($\text{Co } \lambda\text{K}\alpha_1 = 1.78897$ Å). No monochromator or filter was used. The crystallographic studies of the PLD thin-films were done by spinning the sample at 15 rpm. The fingerprint methodology (Phase-ID, search/match routine) was used as a diagnostic tool for the identification of crystal phases and analysis of reaction products. The reference patterns used for the structural analysis were provided in the ICDD Powder Diffraction File database (supplied as PDF-2 and compiled into DIFFRACT^{plus} Reference Database format, released in 2002). Thin-film thicknesses were measured using an XP-2TM profilometer (XP Series Stylus Profilometer, Ambios Technology, Inc.).

The system for evaluating the sensing performance consisted of computer operated elements with a heater (powered using a Xantrex HPD 60-5 power supply), gas-supply manifold with 4 mass flow controllers (MKS Type 1479A), sensing electrodes (gold electrodes connected to a Keithley 2400 sourcemeter) and a custom feedback temperature controller equipped with a K-type thermocouple. For sensing studies, gold electrodes were deposited on the thin-films using a thermal vacuum deposition procedure. In order to assure good ohmic contact, two small pads of gold were placed between the sensing electrodes and the film electrodes. Conductance (resistance) was monitored to detect changes in the electron transport properties with changes in experimental conditions (*e.g.*

temperature effect, interaction with gas-phase species, concentration effects, *etc.*). For the experiments, the total gas flow rate was kept at 250 cm³ / minute (sccm). The temperature range for the sensing functionality studies was between 100 °C and 500 °C. The gases were delivered from certified gas cylinders in appropriate mixtures of O₂ (Linde; 4.5 grade), N₂ (Linde; 5.0 grade) and NO in N₂ (Praxair; nominally 500ppm in ultra N₂). The O₂ exposure studies were done with [O₂] = 0 to 90 % in balance N₂. The NO ranges applied to the sensor were 5 to 400ppm and completed in two sets of measurements. The first set was with 20% O₂ 80% N₂ as the carrier and the second with 100% N₂ as carrier to “bracket” the O₂ concentration ranges expected in exhaust environments. This approach provided a means to assess relative sensor response characteristics to [NO] in the presence of differing O₂ environments.

3. Results and Discussion

3.1 Structural Characterization

Formation of single phase CuWO₄ from the CuO and WO₃ precursors was confirmed by comparing the XRD laser target reflections with database standards (DIFFRACT^{plus} 2002 reference database pattern # 01-088-0269). No reflections from reagents or other reaction products were observed, however peaks due to Co-Kβ radiation are present. **Figure 1** shows the XRD pattern for PLD targets of CuWO₄. An excellent match for reflections were found for the PLD targets and the database standards.

Figure 1. XRD for CuWO₄ PLD target.

Figure 2 shows the XRD for a CuWO₄ thin-film along with the XRD for the CuWO₄ PLD pellet and the XRD for the substrate (α-Al₂O₃). As expected, the thin-film XRD includes the substrate reflections (note that both the substrate (α-Al₂O₃) and the thin-film material (CuWO₄) display XRD patterns with reflections about similar 2θ angles). An overlap at 2θ ≈ 26.9 ° and 62.1 ° occurred. This is supported by a change in the observed order for relative intensity at these 2θ angle (considering

the substrate reflections). The thin-film XRD for the CuWO₄ thin-film displayed a reduced number of reflections compared with the bulk material, indicative of the film having a preferential orientation. The CuWO₄ thin-films thickness estimated by optical profilometry was in the 280 nm range.

Figure 2. XRD for representative thin-film with CuWO₄ composition showing preferential orientations.

3.2 Sensor Functionality Study

The sensing mechanism displayed by semiconducting metal-oxides to redox gas-phase species, including O₂, NO and NO₂, operates by physicochemical interactions originating in the surface of the sensing material (*e.g.* production and consumption of surface defects, electron transfer events, formation of stable adsorbates through chemisorption, in particular formation of oxygen adsorbates and, in general, redox interactions with gas-phase species). The formation of ionized surface adsorbates at the semiconductor surface at the expense of removal of electrons modifies the electronic properties of the interacting surface. The variation in charge carrier concentration and the diversification of the chemical nature of surface-states with both temperature and surrounding gas-phase species result in a measurable change in electrical conductance. It is worth noting that for some cases, there also exist chemical processes in the film bulk that contribute to the transport of electric charge, particularly when ionic migration and transport is possible. Consequently, monitoring changes in the electron transport properties provides information that allows the evaluation of the sensor functionality to target gas-phase species [4-6,11,13,15-20,22]. **Equation 1** summarizes the fundamental process that renders semiconducting metal-oxides suitable for sensing gas-phase species that undergo a redox change upon interaction with surface-states [3-6,8,19-25]. In **Equation 1**, O₀^x represents an unstable lattice oxygen and V_O²⁺, an oxygen vacancy with charge 2+.



3.2.1 Response of CuWO₄ Thin-Films to Temperatures Changes

Figure 3 shows the response to cyclic temperature changes for CuWO₄ thin-films in the 200 - 500 °C temperature range. As expected for a semiconductor, a temperature increase promotes an enhancement in the charge transport, which is evidenced by an increase in electronic conductance (σ) with temperature.

Figure 3. Thermal stability and reproducibility of electrical response (σ) with temperature in synthetic air (20 % O₂ in N₂) for a CuWO₄ thin-film. The rate for temperature change was 2 °C / min.

Despite the thermal stress caused by cyclical temperature changes, the thin-film conductance profile showed good reproducibility ($\pm 6\%$) and signal stability for both the conductance value corresponding to the reference state (20 % O₂ in N₂, T = 200 °C) and those at operating temperatures (300, 400, 500 °C). The reproducible conductance profile indicates that the thin-films possess good mechanical adherence to the substrate and suitable thermal and electrical stability.

3.2.2 Response of CuWO₄ Thin-Films to O₂

In hydrocarbon fuelled engines, the exhaust composition has a dependency upon the rich or lean nature of the combustion mixture. As a result of combustion, the oxygen concentration [O₂] in the exhaust is no longer equal to the [O₂] in the pre-combustion mixture and [O₂] can range from ~20 % in the pre-combustion mixture to close to zero in the exhaust. Thus, the oxygen abundance in the exhaust is a parameter of the operational condition of the engine, so in order to ascertain the CuWO₄ sensor functionality in this application, the electrical response to changing [O₂] was also examined.

Measurements of σ vs. [O₂] at both 300 °C and 500 °C were performed in order to study the effect of O₂ on the conductance of the thin-film, **Figure 4a and 4b**. The plots in **Figure 4** show the effect of increasing O₂-to-N₂ molar ratio at the working temperatures, **4a**. T = 300 °C and **4b**. T = 500 °C. For these experiments, the reference gas was synthetic air (20 % O₂ in N₂). The oxygen concentration is given in molar percentage. The analysis of the plots reveals that conductance values progressively decreased as [O₂] increased. This is the result of a decrease in the concentration of surface electrons (formation of oxygen adsorbates) and the annihilation of oxygen vacancies through

chemical interactions between molecular O₂ and the semiconducting surface (**Equation 1**). Since the conductance values progressively decreased with increasing [O₂] at both operating temperatures, the CuWO₄ thin-films display an n-type conductivity. The monitoring response (defined as 90 % of the conductance value for the steady state response) at 300 °C occurred at exposure periods of ~ 80 - 90 minutes, and at 500 °C, ~ 10 - 12 minutes. At 300 °C, the estimated recovery time (under the reference gas, 20% O₂ in N₂) was approximately 90 minutes, whereas at 500 °C, ~ 10 minutes. The elapsed time to reach the stationary state and the recovery time did not show a significant dependence on [O₂] for either operating temperature.

Figure 4. CuWO₄ thin-film response to O₂ exposure in N₂ (O₂ % = 0 to 90%), T = 300 °C and 500 °C.

Figure 5 displays the response factors \mathcal{R}_f to O₂ for the thin-film at both 300 and 500 °C as a function of pO_2 ($pO_2 \propto [O_2]$). The calculation of the response \mathcal{R}_f was carried out using **Equation 2**, where R_i represents the resistance values with varying [O₂], and R_{ref} , the resistance recorded upon exposure to the reference gas-system (synthetic air, 20% O₂ in N₂). **Figure 5** also indicates the sensitivity factors S_f corresponding to O₂ exposure at both operating temperatures. Here, S_f is the slope of each curve (T = 300 °C and 500 °C), and further can be defined as the limiting increase in analyte concentration ($\partial[O_2]$ or ∂pO_2) that produces a measurable and reproducible change in the instrumental response (conductance / resistance), **Equation 3**. The estimated sensitivity factors S_f at both temperatures feature comparable values, $S_f(300\text{ °C}) = 0.72\text{ atm}^{-1}$ vs. $S_f(500\text{ °C}) = 0.85\text{ atm}^{-1}$. For both fits, the coefficient of determination was $R^2 > 0.99$. The plotted \mathcal{R}_f values were calculated with average values and the bars indicate the estimated errors. .

$$\mathcal{R}_f = \frac{R_i - R_{ref}}{R_{ref}} \quad (2)$$

$$S_f = \left(\frac{\partial \mathcal{R}_f}{\partial [O_2]} \right)_{\Delta [O_2] \rightarrow 0} \quad (3)$$

Figure 5. Response factors \mathcal{R}_f to O₂ exposure in N₂ (O₂ % = 0 to 90 %), T = 300 and 500 °C.

Reliability tests were performed in order to test the reproducibility of the material response to O₂. This produced consistent changes in electrical conductance with [O₂] at both temperatures, with values reproduced within $\pm 5\%$.

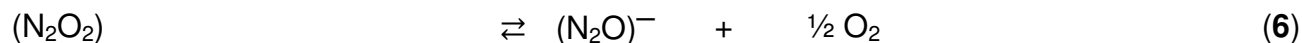
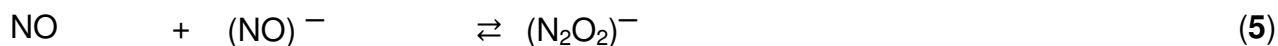
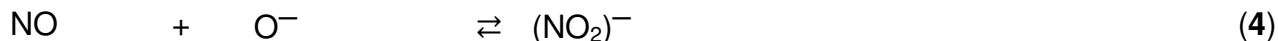
3.2.3 Sensing Performance for CuWO₄ Thin-Films toward Nitrogen Monoxide, T= 300 °C and 500 °C

The sensing functionality to NO was evaluated at both 300 °C and 500 °C with a carrier gas balance of synthetic air (20 % O₂ in N₂) and using the synthetic air resistance level as a reference. NO exposure at 300 °C, **Figure 6**, resulted in an increase in resistance with increasing [NO]. **Figure 6** shows that a steady state was not reached for any of the investigated [NO] within an exposure time of 60 minutes. Therefore, at 300 °C, the sensing response to NO is slow. The recovery of the baseline resistance under the reference gas took $\sim 25 - 30$ minutes.

Figure 6. Sensor response to NO exposure ([NO] range from 19.5 to 370 ppm) at 300 °C. The reference gas system was synthetic air (20% O₂ in N₂). [NO] is indicated in ppm.

The response to NO at 300 °C indicates a decrease in the number of charge carriers (and implies reduction of NO). The set of reactions shown by **Equations 3 - 7** are commonly invoked to explain the sensing mechanism of n-type semiconductor metal-oxides to NO, as has been reported elsewhere [26-34]. In general, the catalytic decomposition of NO on metal-oxide such as TiO₂, CeO₂, WO₃ at T > 100 °C yields N₂O (which further decomposes to N₂ and O₂), N₂ and O₂ (dominant products at T > 900 °C) and, to a lesser extent, NO₂ (which is not produced at T > 500 °C).





Assessment of the sensor functionality to NO was also carried out at 500 °C, **Figure 7**. For this temperature, conversely to that found at 300 °C, NO exposure resulted in an increase in conductance. This response pattern indicates the operation of a different detection mechanism with respect to that at 300 °C, where increasing [NO] produced a decrease in σ . Additionally, in the cases where [NO] > 90 ppm, after an initial fast increase in conductance, there followed a transient of reverse response, **Figure 7**. The transient response is characterized by a fast decrease in electronic conductance. At 500 °C, the sensing response (previously defined as 90 % of the response for the stationary state) occurred within 5 - 8 minutes of NO exposure (estimated for the conductance maximum preceding the evolution of the transient response). The recovery time was approximately 20 minutes for all the NO exposures. The persistent transient response reveals evidence of (at least) two parallel chemical processes in the sensing mechanism.

Figure 7. Sensor response to NO exposure ([NO] range from 19.5 to 390 ppm), T= 500 °C. The reference gas system was synthetic air (20% O₂ in N₂). [NO] is indicated in ppm.

This particular response pattern to NO at high temperatures (increase in σ with [NO]) has been observed before for NO_x monitoring studies using n-type semiconducting metal-oxides [12,35-38]. It is noteworthy that the presence of low concentrations of nitric oxide resulted in an increase in electronic conductance (**Figure 7**), which is the response pattern commonly found for perovskite oxides (p-type materials) when an interaction with oxidizing gases, including molecular O₂, takes place [39]. For instance, the sensing response to NO and NO₂ for both WO₃ and a series of tungstates (MeWO₄, where Me = Mg, Ca, Sr, Ba, Mn, Co, Zn) were investigated in the 450 - 500 °C temperature range [38].

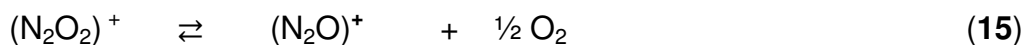
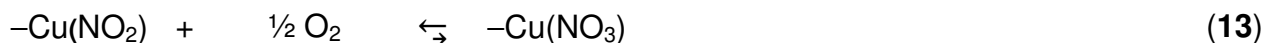
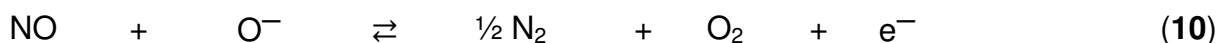
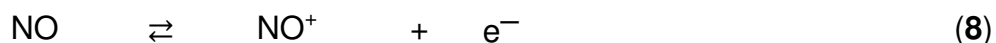
The study reported that the resistance of the thin-film decreased upon exposure to both NO and NO₂ and that response to NO₂ was about 10 times greater than for NO. A transient response upon NO_x exposure was not reported in this research account. Similarly, the physical chemical nature of the transient response has been discussed for the interaction of NO_x with CuO thin-films [35]. Because a rise in electronic conductance often originates from an increase in the concentration of charge carriers [19,22,24-25,28], the combined action of both temperature and chemical interaction between gas-phase species (NO_x) and the thin-film surface could have caused an increase in the concentration of charge carriers (*e.g.* production of oxygen vacancies and surface electrons) [35,37].

To gain insight into the chemical origin of the transient response (**Figure 7**), the response to NO was monitored in absence of molecular O₂ using N₂ as both the background and the reference gas, **Figure 8**. This data, when referenced to that measured in synthetic air, also served the purpose of determining the magnitude of the influence of changing [O₂] on NO sensor response. Surface interaction with NO in N₂ resulted in an increase in the electronic conductance of the thin-film. However, in contrast to the experiments in the presence of molecular O₂ (**Figure 7**), there was no indication of a transient response. This result supports the chief role of molecular O₂ in the sensing events responsible for the observed transient response for NO exposures ([NO] > 90 ppm) in synthetic air at 500 °C (**Figure 7**). At this operating temperature (500 °C), the sensitivity factor to NO in N₂ atmosphere was $S_f(\text{NO}/\text{N}_2) = 1.7 \times 10^{-3} \text{ ppm}^{-1}$. This sensitive factor is comparable to that estimated for NO monitoring in synthetic air $S_f(\text{NO} / 20\% \text{ O}_2 \text{ in N}_2)=2.5 \times 10^{-3} \text{ ppm}^{-1}$. Even though the delta [O₂] is close to the maximum that could be expected in combustion exhaust (*ie* 20% vs 0%) the S_f factors are of the same order. This close agreement in S_f indicates that the low cross-sensitivity to changing [O₂] is a parameter which could, for instance, be conveniently corrected for by using the on-board λ-sensor for evaluation of [O₂] with respect to calculating actual [NO].

Figure 8. Sensor response to NO exposure in N₂ ([NO] range from 100 to 413 ppm), T= 500 °C. [NO] is indicated in ppm.

The response to NO in synthetic air for $[\text{NO}] > 90$ ppm, with the development of a transient signal followed by the progression of the conductivity profile to a smaller and common value of σ , **Figure 7** cannot be subscribed to the isolated interaction between NO_x ($\text{NO} + \frac{1}{2} \text{O}_2 \rightleftharpoons \text{NO}_2$) and the operating surface states because the monitoring experiments took place under steady state conditions. In other words, constant values of $[\text{NO}]$ and $[\text{O}_2]$ with a residence time of 4 minutes does not account for an abrupt decrease in σ . Since the gas-phase formation of NO_2 occurs in parallel to the detection of NO, the effect of NO_2 will not occur isolated in time. Any contribution from NO_2 will add to the measured conductance as it is produced. The increasing concentration of NO in the 97 - 390 ppm range (and the associated increase in $[\text{NO}_2]$ with time) does not account either for a common value of conductance for the steady state situation under NO in synthetic air (**Figure 7**). The origin of the common response to NO (steady state at $\sigma \approx 5.5 \cdot 10^{-7} \Omega^{-1}$) in synthetic air could be related to the formation of surface adducts arising from the interaction of either NO or NO_2 , or both, with thermally excited oxygen lattice atoms or with unstable metallic centers (*e.g.* $-\text{Cu}^{\delta+} \cdots \text{O}^{\delta-}$) followed with a chemical interaction with molecular O_2 . For instance, the formation of a layer of nitrate adducts during NO / synthetic air exposures (*e.g.* $-\text{Cu}(\text{NO}_3)$) would change the electrochemical nature of the sensing surface. The formation of metal nitrates could cause the isolation of the responsive layer of CuWO_4 from the surrounding atmosphere leading to a loss of sensitivity (decrease in electronic conductance). The formation of nitrate species upon interaction of metal-oxide surfaces with NO_x has been reported before for metal oxides such as ZrO_2 [40], Al_2O_3 [41], CeO [29-31], MgO [29], SnO_2 [42], $\text{MoO}_x\text{-SnO}_2$ [42], α - and γ - Fe_2O_3 [43]. In particular, the presence of copper in these phases (*e.g.* CuO , La_2CuO_4 , $\text{Nd}_2\text{CuO}_{4-y}$, Cu-containing zeolites) promotes the formation of nitrate adducts upon interaction with NO_x gases [44-47]. In the case of Cu-containing phases, the formation of nitrates has been linked to a loss in chemical reactivity toward the catalytic decomposition of NO_x gases at high temperatures, which is consistent with the sensitivity loss observed at 500 °C [46,47]. Since metallic nitrates feature relatively low thermal stability, full decomposition of the $-\text{Cu}(\text{NO}_3)$ adducts when NO supply ceases is expected. The decomposition of the nitrate surface adducts

should restore the initial physicochemical properties. A similar situation does not arise at 300 °C, possibly because the formation of nitrate species at the expense of the chemical interaction of NO_x gases with unstable oxygen lattice atoms is not compensated by the available thermal energy. The reaction sequence (**Equations 8 - 15**) intends to represent the chemical origin of the response to NO in synthetic air at 500 °C and the development of a transient response. The proposed reaction step sequence comprises reasonable chemical events within the context of the current data and the data reported in the literature. In **Equation 9**, (O)_x represents a thermally excited oxygen lattice atom. In **Equations 9, 11 and 12**, V_O represents an oxygen vacancy with trapped electrons which can further ionize (*e.g.* V_O ⇌ V²⁺ + 2e⁻) and, in **Equations 11 and 12**, -Cu^{δ+}...O^{δ-} denotes a copper lattice atom bonded to a thermally excited oxygen lattice atom. **Equations 12 - 13** are proposed to account for the transient response observed for [NO] > 90 ppm under synthetic air.



The formation of N₂ and O₂ (**Equation 9, 10 and 15**) were considered since both species are the main products from the catalytic decomposition of NO in metal oxide surfaces (T > 300 °C) [27]. The formation of nitrosyl adducts (NO⁺), which have been proposed as intermediates in the literature [30,48], upon interaction between NO and oxygen vacancies or thermally excited lattice oxygen, **Equation 8 and 9**, is consistent with the surface chemistry of semiconducting metal oxides at high temperature. Catalytic formation of NO₂ at the thin-film surface at T > 500 °C is an endergonic

process and therefore is not considered in this scheme (nonetheless, NO_2 will be produced by the gas-phase reaction between NO and O_2). In this regard, catalytic studies of the chemistry of NO_2 on MgO and CeO_2 surfaces have reported that $(\text{NO}_2)^-$ will not form at $T > 350\text{ }^\circ\text{C}$ [29]. Formation of NO dimers $(\text{N}_2\text{O}_2)^+$, **Equation 14**, has been implied in the catalytic decomposition of NO [32,46-50].

At $500\text{ }^\circ\text{C}$, the operation of two response regimes is also indicated by a well-defined change of slope in the plot of \mathcal{R}_f vs. $[\text{NO}]$ at $[\text{NO}] > 90\text{ ppm}$ (**Figure 9**). A higher sensitivity factor is found in the low $[\text{NO}]$ range; thus, the thin-film displays an enhanced response to NO for $[\text{NO}] < 90\text{ ppm}$. The sensitivity factors S_f at $500\text{ }^\circ\text{C}$ are calculated to be $0.9 \times 10^{-3}\text{ ppm}^{-1}$ for the higher $[\text{NO}]$ concentration range (90 - 390 ppm), and for the lower $[\text{NO}]$ range (19 - 85 ppm), S_f was $2.5 \times 10^{-3}\text{ ppm}^{-1}$. The absence of a transient response for low NO concentrations reinforces the proposed complex mechanism for NO detection.

Figure 9. Response factors vs. $[\text{NO}]$ exposure ($[\text{NO}]$ range from 19.5 to 390 ppm), $T = 500\text{ }^\circ\text{C}$. The reference gas system was synthetic air (20% O_2 in N_2). $[\text{NO}]$ is indicated in ppm.

4. Conclusions

The use of CuWO_4 thin-films deposited by PLD provides conductometric sensor prototypes with response to NO over the range of low ppm to 400ppm concentrations. The similar values of the sensitivity factor, S_f , to NO determined under both an oxygen containing environment (20 % O_2 in N_2 , $S_f(\text{NO}) = 2.5 \times 10^{-3}\text{ ppm}^{-1}$) and under N_2 ($S_f(\text{NO} / \text{N}_2) = 1.7 \times 10^{-3}\text{ ppm}^{-1}$), reveal a low dependence of response to changes in O_2 levels. The NO response can be calibrated to account for changing $[\text{O}_2]$ in exhaust applications by using the on-board λ sensor output signal to give the precise $[\text{O}_2]$. This validates the potential of CuWO_4 thin-films as sensing phases for NO sensor prototypes in combustion exhaust applications. The order for the estimated sensitivity factors to NO in synthetic air ($S_f(\text{NO}) = 2.5 \times 10^{-3}\text{ ppm}^{-1}$, equivalent to $2.5 \times 10^3\text{ atm}^{-1}$) and to O_2 in N_2 ($S_f(\text{O}_2) = 0.85\text{ atm}^{-1}$) also corroborate the enhanced response to NO species that the CuWO_4 phase displays. The CuWO_4 thin-films displayed satisfactory mechanical and thermal endurance. The thermal stability and consistency

of the conductance values with temperature reveal the potential of CuWO₄ thin-films for high-temperature NO monitoring applications. This material showed satisfactory response reproducibility with both temperature and gas-phase analyte. The latter feature indicates that the NO sensing mechanism comprises reversible and temperature-dependent chemical interactions. The opposite response pattern observed for NO detection at 500 °C with respect to the response at 300 °C indicates that surface states play a fundamental role in the detection mechanism of the gas-phase species. At 500 °C, there are two ranges of [NO] (*i.e.* below and above ~ 90ppm) which define regions of differing sensitivity to NO, and are indicative of changing mechanistic drivers.

The higher sensitivity to NO observed for the lower [NO] range at 500 °C indicates the possible use of CuWO₄ thin-films for NO monitoring in the ppm and possibly into the ppb concentration range. An operating temperature of 500 °C is more appropriate for NO sensing in engine exhaust applications.

Acknowledgements

The authors thank the OERD/PERD, NRCan AFTER program for funding support for this work in activity C23.007. This article is recorded as National Research Council of Canada, NRCC# 53072.

Biographies

Carlos M. Gonzalez obtained his B.Sc. in Chemistry (Honors, First Class) from the University of Havana in 1997. He received his Ph.D. degree in Physical Organic Chemistry from Dalhousie University in 2006. Dr. Gonzalez is currently a Research Associate with the National Research Council of Canada. His research focuses on the development of gas sensors prototypes (conductometric sensors) for the monitoring of gas-phase environmental pollutants and the synthesis and physicochemical characterization of semiconducting materials for sensing applications.

Xiaomei Du received her B. Sc degree from the University of Science and Technology Beijing in 1982, and an M.E. degree in Materials Science & Engineering from Beijing University of Aeronautics & Astronautics in 1990. Currently she is a technical officer at the National Research Council of Canada, where her research focuses on chemical sensor materials and technology.

Dr. Jeffrey L. Dunford received his B.Sc. (Mathematics) and B.Sc.H. (Chemistry) from Queen's University in 2001 and 2002, respectively. He completed his M.Sc. and Ph.D. degrees in Physical Chemistry from the University of Toronto in 2003 and 2008, respectively, where he studied the electronic properties of nanostructured materials. Dr. Dunford is currently a Research Associate with the National Research Council of Canada. His research focuses on developing solid-state materials for gas sensors.

Michael Post received his PhD in chemistry from the University of Surrey, UK, and is a Principal Researcher in the Environmental Monitoring Technologies program at the National Research Council of Canada, where he has been an active researcher in materials science since 1975. Current research interests are directed toward the investigation of structural and functional relationships of thin and thick film non-stoichiometric compounds and nanomaterial composites for application as gas sensors.

References

- [1] N. Galloway, F. J Dentener, D. G Capone, E. W. Boyer, R. W. Howarth, S. P. Seitzingers, G. P. Asner, C. C. Cleveland, P. A. Green, E. A. Holland, D. M. Karl, A. F. Michael, J. H. Porter, A. R. Townsend, C. J. Vörösmarty, Nitrogen cycles: past, present, and future, *Biogeochemistry* 70 (2004) 153-226.
- [2] <http://www.epa.gov/airquality/nitrogenoxides/index.html>.
- [3] F. Ménil, V. Coillard, C. Lucat, Critical review of nitrogen monoxide sensors for exhaust gases of lean burn engines, *Sens. and Actuators B* 6 (2000) 1-23.

- [4] D. K. Aswal, S. K. Gupta, Science and Technology of Chemiresistors Gas Sensors, Nova Science Publishers, 2007.
- [5] G. Korotcenkow, Chemical Sensors, Fundamentals of Sensors Materials (Volume 2). Momentum Press, LLC, 2010.
- [6] J. W. Fergus, Materials for high temperature electrochemical NO_x gas sensors, Sens. and Actuators B 121 (2007) 652-663.
- [7] J. Yoo, D. Oh, E. D. Wachsman, Investigation of WO₃-based potentiometric sensor performance (M/YSZ/WO₃, M = Au, Pd, and TiO₂) with varying counter electrode, Solid State Ionics 179 (2008) 2090-2100.
- [8] M. Akiyama, Z. Zhang, J. Tamaki, N. Miura, N. Yamazoe, H. Noboru, Tungsten oxide-based semiconductor sensor for detection of nitrogen oxides in combustion exhaust, Sens. and Actuators B 14 (1993) 619–620.
- [9] L. Chen, S.C. Tsang, Ag doped WO₃-based powder sensor for the detection of NO gas in air, Sens. and Actuators B 89 (2007) 68–75.
- [10] H. Kawasaki, T. Ueda, Y. Suda, T. Ohshima, Properties of metal doped tungsten oxide thin films for NO_x gas sensors grown by PLD method combined with sputtering process, Sens. and Actuators B 100 (2004) 266-269.
- [11] J. Kukkola, J. Mäklin, N. Halonen, T. Kyllönen, Géza Tóth, Maria Szabó, A. Shchukarev, J.-P. Mikkola, H. Jantunen, K. Kordás, Gas sensors based on anodic tungsten oxide, Sens. and Actuators B 153 (2011) 293-300.
- [12] K. Shimizu, K. Kashiwagi, H. Nishiyama, S. Kakimoto, S. Sugaya, H. Yokoi, A. Satsuma, Impedancemetric gas sensor based on Pt and WO₃ co-loaded TiO₂ and ZrO₂ as total NO_x sensing materials, Sens. and Actuators B 130 (2008) 707-712.
- [13] M. Fleischer, H. Meixner, Fast gas sensors based on metal oxides which are stable at high temperatures, Sens. and Actuators B 43 (1997) 1-10.

- [14] D.-S. Lee, S.-D. Han, J.-S. Huh, D.-D. Lee, Nitrogen oxides sensing characteristics of WO₃-based nanocrystalline thick film gas sensor, *Sens. and Actuators B* 60 (1999) 57-63.
- [15] G. Korotcenkov, Gas response control through structural and chemical modification of metal oxide films: state of the art and approaches, *Sens. and Actuators B* 107 (2005) 209-232.
- [16] D. Baresel, W. Gellert, W. Sarholz, P. Scharner, Influence of catalytic activity on semiconducting metal oxide sensors. I. Experimental sensor characteristics and their qualitative interpretation, *Sens. and Actuators* 6 (1984) 35-50.
- [17] G. Korotcenkov, Metal oxides for solid-state gas sensors: what determines our choice? *Mater. Sci. Eng., B* 139 (2007) 1-23.
- [18] V.E. Bochenkov, G.B. Sergeev, Preparation and chemiresistive properties of nanostructured materials, *Adv. Colloid Interface Sci.* 116 (2005) 245-254.
- [19] J. Bardeen, Surface states and rectification at a metal semi-conductor contact, *Phys. Rev.* 71 (1947) 717-727.
- [20] H. Meixner, J. Gerblinger, U. Lampe, M. Fleischer, Thin-film gas sensors based on semiconducting metal oxides, *Sens. and Actuators B* 23 (1995) 119-125.
- [21] G. Pacchioni, Oxygen vacancy: the invisible agent on oxide surfaces, *Chem. Phys. Chem.* 4 (2003) 1041-1047.
- [22] V.E. Bochenkov, G.B. Sergeev, Preparation and chemiresistive properties of nanostructured materials, *Adv. Colloid Interface Sci.* 116 (2005) 245-254.
- [23] H. Statz, G. A. Demars, Electrical conduction via slow surface states on semiconductors, *Phys. Rev.* 111 (1958) 169-182.
- [24] M. Batzill, U. Diebold, The surface and materials science of tin oxide, *Prog. Surf. Sci.* 79 (2005) 47-154.
- [25] J. Ding, T.J. McAvoy, R.E. Cavicchi, S. Semancik, Surface state trapping model for SnO₂-based microplate sensor, *Sens. Actuators B* 77 (2001) 597-613.

- [26] C. S. Rout, K. Ganesh, A. Govindaraj, C. N. R. Rao, Sensors for the nitrogen oxides, NO₂, NO and N₂O, based on In₂O₃ and WO₃ nanowires, *Appl. Phys. A* 85 (2006), 241-246.
- [27] J. M. Fraser, F. Daniels, The heterogeneous decomposition of nitric oxide with oxide catalysts, *J. Phys. Chem.* 62 (1958) 215-219.
- [28] T. J. Dines, C. H. Rochester, A. W. Ward, Infrared and raman study of the adsorption of NH₃, pyridine, NO and NO₂, on anatase, *J. Chem. Soc. Faraday Trans.* 87 (1991) 643-651.
- [29] J. A. Rodriguez, T. J. Jirsak, Chemistry of NO₂ on CeO₂ and MgO: experimental and theoretical studies on the formation of NO₃, *Chem. Phys.* 112 (2000) 9929-9939.
- [30] G. Li, K. Kaneko, S. Ozeki, Chemisorption and photoadsorption of NO on cerium(IV) oxide, *Langmuir* 13 (1997) 5894-5899.
- [31] M. Niwa, Y. Furukawa, Y. Murakami, Adsorption of nitric oxide on cerium oxide, *J. Colloid Interface Sci.* 86 (1982) 260-265.
- [32] D. C. Sorescu, C. N. Rusu, J. T. Yates, Adsorption of NO on the TiO₂ (110) surface: an experimental and theoretical study, *J. Phys. Chem. B*, 104 (2000) 4408-4417.
- [33] M. Iwamoto, H. Hamada, Removal of nitrogen monoxide from exhaust gases through novel catalytic processes, *Catal. Today* 10 (1991) 57-71.
- [34] T. Sakata, Y. Yoneda. The catalytic decomposition of nitrogen monoxide over supported platinum catalyst, *Nippon Kagaku Kaishi* 6 (1978) 791-798.
- [35] Y.-S. Kim, I.-S. Hwang, S.-J. Kim, Ch.-Y. Lee, J.-H. Lee, CuO nanowire gas sensors for air quality control in automotive cabin, *Sens. and Actuators B* 135 (2008) 298-303.
- [36] G. Williams, G. S. V. Coles, NO_x response of tin dioxide based gas sensors, *Sens. and Actuators B* 15-16 (1993) 349-353.
- [37] G. Sberveglieri, S. Grappeli, P. Nelli, Highly sensitive and selective NO_x and NO₂ sensors based on Cd-doped SnO₂ thin film, *Sens. and Actuators* 4 (1991) 457-461.

- [38] J. Tamaki, T. Fujii, K. Fujimori, N. Miura, N. Yamazoe, Application of metal tungstate-carbonate composite to nitrogen oxides sensor operative at elevated temperature, *Sens. and Actuators B* 25 (1995) 396-399.
- [39] M. A. Peña, J. L. G. Fierro, Chemical structures and performance of perovskite oxides, *Chem. Rev.* 101 (2001) 1981-2017.
- [40] K. Hadjiivanov, Use of overtones and combination modes for the identification of surface NO_x anionic species by IR spectroscopy, *Catal. Lett.* 68 (2000) 157-161.
- [41] E. Ozensoy, C. H. F. Peden, J. Szanyi, NO_2 adsorption on ultrathin $\theta\text{-Al}_2\text{O}_3$ films: formation of nitrite and nitrate species, *J. Phys. Chem. B.* 109 (2005) 15977-15984.
- [42] A. Chiorino, G. Ghiotti, F. Prinetto, M.C. Carotta, D. Gnani, G. Martinelli, Preparation and characterization of SnO and $\text{MoO}_x - \text{SnO}_2$ nanosized powders for thick film gas sensors, *Sens. Actuators B.* 58 (1999) 338-349.
- [43] B. C. Hixson, J. W. Jordan, E. L. Wagner, H. M. Bevsek, Reaction products and kinetics of the reaction of NO_2 with $\gamma\text{-Fe}_2\text{O}_3$, *J. Phys. Chem. A.* 115 (2011) 13364-13369.
- [44] F.M. Van Assche IV, E. D Wachsman, Isotopically labeled oxygen studies of the NO_x exchange behavior of La_2CuO_4 to determine potentiometric sensor response mechanism, *Solid State Ionics* 179 (2008) 2225-2233.
- [45] K.-Y. Ho, M. Miyayama, Y. Hiroaki, NO_x gas responding properties of $\text{Nd}_2\text{CuO}_{4-y}$ thick film, *Mater. Chem. Phys.* 49 (1997) 7-11.
- [46] G. Centi, S. Perathoner, Nature of active species in copper-based catalysts and their chemistry of transformation of nitrogen oxides, *Appl. Catal. A: General* 132 (1995) 179-259.
- [47] G. Centi, S Perathoner, Role and importance of oxidized nitrogen oxide adspecies on the mechanism and dynamics of reaction over copper-based catalysts, *Catal. Today* 2 (1996) 117-122.

- [48] S. Furuyama, T. Morimoto, R. Hirasawa, Heat of dissociation of nitric oxide adsorbed on magnesium oxide determined by the electron spin resonance technique, *J. Phys. Chem.* 82 (1978) 1027-1028.
- [49] W. F. Schneider, K. C. Hass, M. Miletic, J. L. Gland, Dramatic cooperative effects in adsorption of NO_x on MgO (001), *J. Phys. Chem. B* 106 (2002) 7405-7413.
- [50] Z.-M. Wang, T. Arai, M. Kumagai, Cooperative and competitive adsorption mechanism of NO₂, NO, and H₂O on H-type mordenite, *Ind. Eng. Chem. Res.* 40 (2001) 1864-1871.